JOURNAL OF SOLID STATE CHEMISTRY **111**, 427–436 (1994)

Oxyfluorinated Microporous Compounds

V. Synthesis and X-Ray Structural Determination of ULM-3, a New Fluorinated Gallophosphate $Ga_3P_3O_{12}F_2$, $H_3N(CH_2)_3NH_3$, H_2O

Thierry Loiseau, Richard Retoux, Philippe Lacorre, and Gérard Férey[1]

Laboratoire des Fluorures, URA CNRS 449, Faculté des Sciences, Université du Maine, Avenue Olivier Messiaen, 72017 Le Mans Cedex, France

Received June 7, 1993; accepted November 10, 1993

$Ga_3P_3O_{12}F_2$, $H_3N(CH_2)_3NH_3$, H_2O was obtained by hydrothermal synthesis (453 K, 24 hr, autogeneous pressure) from a mixture of Ga_2O_3, P_2O_5, HF, 1,3-diaminopropane, and H_2O in the ratio 1 : 1 : 2 : 1.3 : 80. It is orthorhombic (space group *Pbca* (No. 61) with $a = 10.154(1)$ Å, $b = 18.393(2)$ Å, $c = 15.773(2)$ Å, $V = 2945.8(9)$ Å^3, $Z = 8$. The three-dimensional network is built up from corner-linked $[Ga_3(PO_4)_3F_2]$ units composed of three PO_4 tetrahedra, two GaO_4F trigonal bipyramids, and one GaO_4F_2 octahedron. Fluorine atoms are shared between the octahedron and the bipyramid. The framework delimits 10-membered ring channels along [100] and 8-membered ones along [101] and [10−1]. The amine and the water molecule are inserted in the 10-membered ring channels. The hydrogen bonding scheme is discussed and shows that the water is principally linked to the amine within the tunnel and that the template might be the amine monohydrate. The thermal behavior of the title compound is studied by TGA and X-ray thermodiffractometry. © 1994 Academic Press, Inc.

INTRODUCTION

Since the discovery of a new series of microporous aluminophosphates $AlPO_4$-*n* (1), synthesized by using organic amines or quaternary ammoniums cations as templates, numerous phosphate-based molecular sieves have been reported (2–4 and references therein). Several years ago, Guth *et al.* (5) developed a new route of synthesis in the presence of fluorine. The addition of fluoride ions in the reaction medium seems to induce mineralization and allows the crystallization of zeolites at neutral or acidic pH and the partial substitution (6) of silicon by other metals such as B^{3+}, Al^{3+}, Ga^{3+}, Fe^{3+}, Ge^{4+}, and Ti^{4+}. Moreover, as encountered in many phases (7), fluorine is also incorporated into the open frameworks. The best example is cloverite (8), with three-dimensional 20-membered ring channels, in which the fluorine is located at the center of a double four-ring (D4R) cage. The same configuration surrounding fluorine is observed in other compounds such as the pure-silica octadecasil (AST) (9) or the LTA-type $GaPO_4$ (7).

Recently, we focused attention on the synthesis of new fluorinated alumino- and gallophosphates (10–13) in the systems M_2O_3 (M = Al, Ga)–P_2O_5–HF–template–H_2O. In these phases, which we propose labeling ULM-*n* (for University of Le Mans), the case of fluorine is different since it is directly involved in the coordination sphere of M, as also observed in $GaAsO_4$-2 (14). We report here the preparation and characterization of a new phase $Ga_3P_3O_{12}F_2$, $H_3N(CH_2)NH_3$, H_2O, synthesized with 1,3-diaminopropane (hereafter noted DAP) as template.

EXPERIMENTAL

Synthesis

The title compound was prepared by hydrothermal synthesis under autogeneous pressure. The reactants were gallium oxide (Ga_2O_3, Merck 99%+), phosphoric acid (85% H_3PO_4, Prolabo RP Normapur), hydrofluoric acid (40% HF, Prolabo RP Normapur), and 1,3-diaminopropane ($H_2N(CH_2)_3NH_2$, Aldrick 99%+). The starting mixture corresponding to the molar composition 1 Ga_2O_3, 1 P_2O_5, 2 HF, 1.3 DAP, and 80 H_2O was placed without stirring in a Teflon-lined stainless-steel autoclave, heated at 453 K for 24 hr and then cooled to room temperature for 24 hr. The pH of the synthesis rises from 1–2 before heating to 5 at the end of the reaction. The obtained crystalline product was filtered off, washed with distilled water, and dried at room temperature. Its calculated X-ray powder diffraction pattern is reported in Table 1.

Structure Determination

A parallelepipedic-shaped single crystal was selected from the sample for structural analysis by X-ray diffrac-

---

[1] To whom correspondence should be addressed.

0022-4596/94 $6.00

TABLE 1

Calculated Interplanar *d*-Spacings (Å) and Calculated Normalized Intensities for $Ga_3(PO_4)_3F_2$, H_2O, $H_3N(CH_2)_3NH_3$

h k l	d_{calc}	I_{calc}
0 2 0	9.20	76
0 2 1	7.94	28
0 0 2	7.89	100
1 1 1	7.74	45
1 1 2	5.90	47
2 0 0	5.08	16
0 4 0	4.598	6
1 1 3	4.525	7
2 2 0	4.445	9
0 4 1	4.415	8
2 0 2	4.269	7
1 4 1	4.048	10
0 0 4	3.943	7
1 3 3	3.715	25
0 4 3	3.461	5
1 5 1	3.378	15
3 1 1	3.257	17
1 5 2	3.167	5
2 1 4	3.071	16
3 1 2	3.067	31
0 2 5	2.984	17
1 1 5	2.973	6
1 5 3	2.889	14
1 6 1	2.885	6
0 6 2	2.857	12
1 6 2	2.750	6
3 3 3	2.581	6
1 0 6	2.545	6
3 5 1	2.460	16
3 5 3	2.251	14

tion. Its quality was tested by optical observation and Laue photographs. Intensity data collection was performed with a Siemens AED-2 four-circle diffractometer with conditions of data collection summarized in Table 2 and allowed a description of the structure in the space group *Pbca* (No. 61). The data were corrected for Lorentz polarization and absorption effects. The scattering factors and anomalous dispersion corrections were taken from the "International Tables for X-ray Crystallography" (15). The structure was solved by using the direct method analysis of the SHELXS-86 program (16). Gallium and phosphorus atoms were first located and all the remaining atoms except hydrogens of the water molecule were found by difference Fourier maps. Refinement was performed by full-matrix least-squares analysis of SHELX-76 (17) with anisotropic thermal parameters for all nonhydrogen atoms and with strains on C–H and N–H distances. The location of the fluorine atoms was deduced from preliminary solid-state NMR measurements (18), the anisotropic thermal prameters, the absence in the difference Fourier maps of any residue due to hydrogen atoms (of OH groups) close to the corresponding atoms, and valence bond calculations (19). The reliability factors converge to $R_w = 0.026$ and $R = 0.024$. The atomic coordinates with anisotropic thermal parameters and selected bond distances and angles are listed in Tables 3a, 3b, and 4, respectively. Table 5 provides the valence bond analysis of the structure. The list of structure factors can be obtained upon request to the authors.

Thermal Analysis

TGA measurements were performed on a Perkin–Elmer thermoanalyzer under argon gas flow with a heating rate of 5°C/min between 300 and 973 K. The X-ray thermodiffractometry experiment was carried out under helium flow on a Siemens D5000 diffractometer (θ/θ configuration) equipped with a PSD (Elphyse) and a high-temperature attachment Anton Parr HTK10, using $Co(K\alpha_1 + K\alpha_2)$ radiation, 20 sec per degree (θ) and a step size of 0.03° 2θ. The powder patterns were collected every 10°, between 300 and 973 K, in the angular range $10° < 2\theta < 70°$. The heating procedure between each step was as follows: heating at 6°/min, 5 min at the desired temperature, and then collection of the data at this temperature.

RESULTS AND DISCUSSION

Description of the Structure

In this new structure type, the three types of phosphorus atoms are in a nearly regular tetrahedral surrounding with P–O distances within 1.525–1.556 Å. The gallium atoms present two different coordinations: Ga(1) is octahedrally coordinated with four oxygen (Ga(1)–O_{av} = 1.956 Å) and two fluorine atoms (Ga(1)–F_{av} = 1.956 Å). The polyhedra around Ga(2) and Ga(3) are distorted trigonal bipyramids with a distance between Ga and F (1.99 Å) longer than that between Ga and O (1.835–1.983 Å for Ga(2) and 1.860–1.937 Å for Ga(3)). The two types of gallium polyhedra are linked together via the fluorine atoms and the resulting trimers $Ga_3O_{12}F_2$ of gallium polyhedra (two trigonal bipyramids and one octahedron) are separated from each other by phosphorus tetrahedra. The association of the three types of phosphorus tetrahedra with the previously defined trimers leads to the basic asymmetric unit $[Ga_3(PO_4)_3F_2]^{2-}$ (Fig. 1).

The three-dimensional network is built up from the link-

TABLE 2

Conditions of the X-Ray Data Collection of $Ga_3P_3O_{12}F_2$, H_2O, $H_3N(CH_2)_3NH_3$

Determination of cell parameters	32 reflections at $2\theta \approx 30°$
Space group	*Pbca* (No. 61)
Cell dimensions	$a = 10.154(1)$ Å
	$b = 18.393(2)$ Å
	$c = 15.773(2)$ Å
Volume/Z	2945.8(9) $Å^3/Z = 8$
Wavelength/monochromator	0.71073 Å (Mo $K\alpha$)/graphite
Temperature	293 K
Scan mode	ω-2θ
Step scan	$37 \leq N \leq 43$, every 0.035° and 4 sec
Aperture	3.5×3.5 mm^2
Crystal dimensions	$0.342 \times 0.110 \times 0.091$ mm^3
Natural faces	{100}, {010}, {001}
Absorption corrections	Gaussian method
Transmission factors	$T_{min} = 0.530$, $T_{max} = 0.608$
Absorption coefficient	$\mu = 58.1$ cm^{-1}
Angular range of data collection	$2\theta \leq 70°$
Range of measured h, k, l	$0 \leq h \leq 16$, $0 \leq k \leq 25$, $0 \leq l \leq 30$
Standard reflections (3)	0 2 10; −3 −8 1, 4 −6 0
Measured every	60 mn
Measured reflections	7175
Independent ref. ($\lvert F\rvert > 6\sigma(\lvert F\rvert)$)	3928
Weight	$w = 0.990/(\sigma^2(F) + 0.000495F^2)$
Secondary extinction	$X = 3.0 \times 10^{-7}$
Number of refined parameters	275
Final Fourier residuals	−0.61 to 0.72 $e \cdot Å^{-3}$
R_w/R	0.026/0.024

age of these units and occurs via corners occupied by oxygens shared by both gallium and phosphorus atoms. The connection of the asymmetric units is shown in Figs. 2a to 2c. Crosslinked 10- and 8-membered channels are then formed along [100] and ([101] + [10−1]), respectively, with a strict Ga–P alternation in the polyhedra forming the channel. The free aperture dimensions of the largest channel are indicated in Fig. 3. The DAP and the

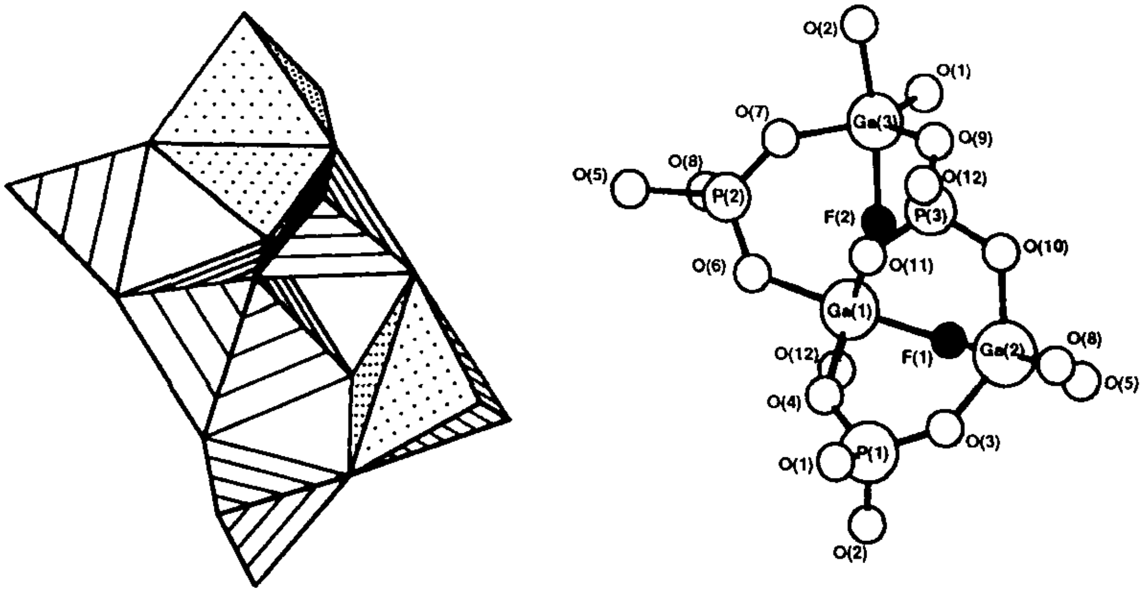

FIG. 1. Polyhedral and ball and stick model of the asymmetric unit. The labels of atoms are given in Table 3.

water molecules are located in the 10-ring channels (Fig. 2a and Fig. 4). The amine is protonated twice and balances the two negative charges of the framework. Its configuration is represented in Fig. 5. Examination of the hydrogen bond scheme between the encapsulated species and the skeleton shows that the strongest hydrogen bond (O(w)–H(12)) exists within the tunnel between one hydrogen of the N(2) amino group and the oxygen of the water molecule (see Table 4). This seems to indicate the existence under our experimental conditions of a monohydrate of DAP, which might be the real templating agent in this structure. The other hydrogen bonds occur between the hydrogens of each amino group of DAP and some oxygen or fluorine atoms of the framework, as also shown in Fig. 5.

Thermal Behavior

The TGA curve (Fig. 6) indicates a two-step behavior. Water is lost between 25 and 205°C (weight loss, 2.9% exp., 2.87% calc.). The amine begins to leave the structure above 205°C; it is completely evolved at 670°C. In the X-ray diffraction pattern of the residue, the same main diffraction peaks as those of the starting material are present, albeit broadened and with weaker intensities; the background is higher. For a better understanding of the thermal decomposition of our phase, a preliminary and qualitative thermodiffractometric study was undertaken. The thermal evolution of the diffraction pattern (Fig. 7) shows modifications which can be correlated with those observed in the TGA measurements, with a shift in the temperatures due to the different heating treatments. This technique makes it possible to follow the evolution of the cell parameters during the heating process and to witness phase transitions and, in the best cases, the evolution of the structure. Figure 7 clearly shows three domains, donated I, II, III: (i) at low temperature, the diffraction peaks of the original hydrated phase remain practically unchanged, except for a very slight shift due to thermal expansion; (ii) at intermediate temperature, after an abrupt change in cell parameters corresponding to a decrease in the cell volume partly due to the loss of water, the diffraction pattern of the dehydrated phase seems almost similar in nature to that of the starting material; (iii) at high temperature, after a phase transition related to the department of the amine, the diffraction pattern of the resulting material exhibits a resemblance with that of the parent structure, despite a loss of crystallinity, with most of the strong peaks still present. The fit of the cell parameters makes it possible to define more accurately the two first domains. Figure 8 shows the evolution. Up to 373 K, the hydrated form is preserved, with a slight thermal expansion of *a* and *c* parameters, while *b* remains constant. The loss of the water molecule gives rise to a sharp decrease in *a* and *b* parameters and a small decrease in *c*. The dehydration is achieved at 423 K. The anhydrous phase is stable in the range 423–513 K. Above the last temperature, strong modification of the lines prevents from giving accurate conclusions on the phase transition. Quantitative experiments for a structure identification of the high-temperature phase using the Rietveld method are currently in progress.

TABLE 3a

Atomic Coordinates and Equivalent Isotropic Factors in $Ga_3P_3O_{12}F_2$, H_2O, $H_3N(CH_2)_3NH_3$

	x	y	z	B_{eq} (Å^2)
Ga(1)	0.1801(1)	0.7179(1)	0.5381(1)	0.60(1)
Ga(2)	0.1634(1)	0.3260(1)	0.8512(1)	0.63(1)
Ga(3)	0.1490(1)	0.5943(1)	0.0036(1)	0.6091)
P(1)	0.1405(1)	0.0759(1)	0.5164(1)	0.57(2)
P(2)	0.3495(1)	0.1683(1)	0.1845(1)	0.59(2)
P(3)	0.1204(1)	0.1830(1)	0.9372(1)	0.61(2)
F(1)	0.3267(2)	0.3142(1)	0.9193(1)	1.23(6)
F(2)	0.0844(2)	0.6961(1)	0.0014(1)	1.36(6)
O(1)	0.0011(2)	0.4334(1)	0.0555(1)	0.79(6)
O(2)	0.2140(2)	0.4963(1)	0.0198(1)	0.94(6)
O(3)	0.1208(2)	0.4010(1)	0.9232(1)	1.05(7)
O(4)	0.2154(2)	0.3668(1)	0.0686(1)	0.76(6)
O(5)	0.2648(2)	0.1462(1)	0.2606(1)	1.01(7)
O(6)	0.3164(2)	0.2454(1)	0.1546(1)	0.97(6)
O(7)	0.3139(2)	0.1100(1)	0.1180(1)	0.89(6)
O(8)	0.4950(2)	0.1618(1)	0.2105(1)	0.88(6)
O(9)	0.7086(2)	0.3855(1)	0.0686(1)	0.92(6)
O(10)	0.6403(2)	0.2742(1)	0.1462(1)	0.98(7)
O(11)	0.6569(2)	0.2708(1)	0.9858(1)	0.79(6)
O(12)	0.4770(2)	0.3418(1)	0.0558(1)	0.96(7)
O(w)	0.0160(4)	0.3012(2)	0.1816(2)	4.6(2)
N(1)	0.5333(3)	0.4113(2)	0.8713(2)	2.0(1)
N(2)	0.3262(4)	0.1120(2)	0.7434(3)	3.4(2)
C(1)	0.5142(4)	0.9876(2)	0.6332(3)	2.9(2)
C(2)	0.3606(5)	0.0339(2)	0.7513(3)	3.1(2)
C(3)	0.4994(4)	0.0190(3)	0.7209(3)	3.0(2)
H(1)	0.460(5)	0.015(3)	0.594(3)	3.8(2)
H(2)	0.607(3)	0.983(3)	0.620(4)	3.8(2)
H(3)	0.297(4)	0.007(3)	0.718(3)	3.8(2)
H(4)	0.363(6)	0.028(3)	0.813(2)	3.8(2)
H(5)	0.541(5)	0.066(2)	0.725(3)	3.8(2)
H(6)	0.529(5)	0.989(3)	0.767(3)	3.8(2)
H(7)	0.626(2)	0.411(3)	0.874(4)	3.8(2)
H(8)	0.479(5)	0.390(3)	0.914(3)	3.8(2)
H(9)	0.507(5)	0.392(3)	0.818(2)	3.8(2)
H(10)	0.258(4)	0.123(3)	0.783(3)	3.8(2)
H(11)	0.334(5)	0.121(3)	0.685(2)	3.8(2)
H(12)	0.396(4)	0.132(3)	0.776(3)	3.8(2)

Note. B_{eq} is defined as $B_{eq} = 8\pi^2(U_{11} + U_{22} + U_{33})/3$.

TABLE 3b
Anisotropic Thermal Parameters in $Ga_3P_3O_{12}F_2$, H_2O, $H_3N(CH_2)_3NH_3$ ($U_{ij}\times 10^4$)

	U_{11}	U_{22}	U_{33}	U_{23}	U_{13}	U_{12}
Ga(1)	68(1)	66(1)	94(1)	2(1)	10(1)	9(1)
Ga(2)	88(1)	79(1)	73(1)	2(1)	10(1)	−7(1)
Ga(3)	62(1)	77(1)	87(1)	−10(1)	0(1)	−13(1)
P(1)	64(2)	59(2)	94(2)	7(2)	−9(2)	−5(2)
P(2)	70(2)	81(2)	73(2)	5(2)	2(2)	2(2)
P(3)	62(2)	64(2)	105(3)	4(2)	−4(2)	4(2)
F(1)	129(7)	200(8)	139(7)	42(6)	−21(6)	−12(6)
F(2)	158(8)	120(7)	239(9)	−7(7)	−31(7)	0(6)
O(1)	59(7)	107(8)	133(8)	−21(7)	−3(6)	1(6)
O(2)	91(7)	67(8)	198(10)	0(7)	−16(7)	−9(6)
O(3)	168(9)	125(9)	105(8)	−36(7)	−38(7)	49(7)
O(4)	106(8)	78(7)	107(8)	−4(6)	−11(6)	31(6)
O(5)	117(8)	159(9)	109(8)	−4(7)	59(7)	−8(7)
O(6)	172(8)	83(8)	111(8)	−3(7)	−32(7)	22(7)
O(7)	138(8)	109(8)	92(8)	−15(6)	11(7)	−24(7)
O(8)	65(7)	142(9)	127(8)	20(7)	0(6)	−1(6)
O(9)	99(8)	83(8)	168(9)	−22(7)	44(7)	−30(6)
O10)	176(9)	99(8)	98(8)	16(6)	9(7)	17(7)
O(11)	80(7)	112(8)	109(8)	−35(6)	1(6)	2(6)
O(12)	65(7)	98(8)	203(10)	−28(7)	−11(7)	14(6)
O(w)	536(23)	714(27)	489(21)	339(19)	176(17)	230(20)
N(1)	218(13)	264(15)	272(14)	2(12)	−9(11)	−13(11)
N(2)	423(21)	348(19)	509(24)	58(18)	29(19)	100(17)
C(1)	320(20)	289(19)	477(24)	27(17)	86(18)	−76(16)
C(2)	379(22)	316(20)	463(25)	−46(19)	38(19)	−76(17)
C(3)	310(20)	310(20)	533(27)	−111(19)	−71(19)	−18(17)

TABLE 4
Selected Interatomic Distances (Å) and Angles (°) in $Ga_3P_3O_{12}F_2$, H_2O, $H_3N(CH_2)_3NH_3$

P(1))$_4$ tetrahedron

P(1)–O(2)	1.525(3)	O(4)–P(1)–O(2)	109.6(1)
P(1)–O(4)	1.540(2)	O(3)–P(1)–O(2)	109.7(1)
P(1)–O(3)	1.544(2)	O(1)–P(1)–O(2)	109.7(1)
P(1)–O(1)	1.556(2)	O(3)–P(1)–O(4)	112.7(1)
		O(1)–P(1)–O(4)	108.3(1)
		O(1)–P(1)–O(3)	106.8(1)

P(2)O$_4$ tetrahedron

P(2)–O(6)	1.532(3)	O(5)–P(2)–O(6)	1113(1)
P(2)–O(5)	1.533(2)	O(8)–P(2)–O(6)	111.4(1)
P(2)–O(8)	1.540(2)	O(7)–P(2)–O(6)	112.5(1)
P(2)–O(7)	1.544(2)	O(8)–P(2)–O(5)	108.1(1)
		O(7)–P(2)–O(5)	102.5(1)
		O(7)–P(2)–O(8)	110.6(1)

P(3)O$_4$ tetrahedron

P(3)–O(11)	1.528(2)	O(12)–P(2)–O(11)	109.8(1)
P(3)–O(12)	1.532(2)	O(10)–P(2)–O(11)	111.2(1)
P(3)–O(10)	1.547(2)	O(9)–P(2)–O(11)	111.0(1)
P(3)–O(9)	1.550(3)	O(10)–P(2)–O(12)	109.7(1)
		O(9)–P(2)–O(12)	108.2(1)
		O(9)–P(2)–O(10)	106.7(1)

TABLE 4—*Continued*

Ga(1)O_4F_2 octahedron

Ga(1)–F(2)	1.946(3)	O(4)–Ga(1)–F(2)	176.0(1)
Ga(1)–O(4)	1.947(3)	O(6)–Ga(1)–F(2)	90.4(1)
Ga(1)–O(12)	1.959(2)	O(12)–Ga(1)–F(2)	95.2(1)
Ga(1)–O(6)	1.959(2)	O(11)–Ga(1)–F(2)	87.8(1)
Ga(1)–O(11)	1.959(2)	F(1)–Ga(1)–F(2)	86.7(1)
Ga(1)–F(1)	1.967(2)	O(6)–Ga(1)–O(4)	92.0(1)
		O(12)–Ga(1)–O(4)	87.8(1)
		O(11)–Ga(1)–O(4)	89.0(1)
		F(1)–Ga(1)–O(4)	90.8(1)
		O(12)–Ga(1)–O(6)	94.3(1)
		O(11)–Ga(1)–O(6)	89.7(1)
		F(1)–Ga(1)–O(6)	177.1(1)
		O(11)–Ga(1)–O(12)	175.0(1)
		F(1)–Ga(1)–O(12)	86.5(1)
		F(1)–Ga(1)–O(11)	89.7(1)

Ga(2)O_4F trigonal bipyramid

Ga(2)–O(5)	1.835(2)	O(3)–Ga(1)–O(5)	113.9(1)
Ga(2)–O(3)	1.839(3)	O(10)–Ga(2)–O(5)	111.4(1)
Ga(2)–O(10)	1.859(3)	O(8)–Ga(2)–O(5)	94.1(1)
Ga(2)–O(8)	1.983(2)	F(1)–Ga(2)–O(5)	89.0(1)
Ga(2)–F(1)	1.990(2)	O(10)–Ga(2)–O(3)	134.5(1)
		O(8)–Ga(2)–O(3)	90.8(1)
		F(1)–Ga(2)–O(3)	86.8(1)
		O(8)–Ga(2)–O(10)	90.8(1)
		F(1)–Ga(2)–O(10)	89.2(1)
		F(1)–Ga(2)–O(8)	176.7(1)

Ga(3)O_4F trigonal bipyramid

Ga(3)–O(1)	1.860(2)	O(7)–Ga(3)–O(1)	133.9(1)
Ga(3)–O(7)	1.867(2)	O(9)–Ga(3)–O(1)	112.5(1)
Ga(3)–O(9)	1.880(2)	O(2)–Ga(3)–O(1)	95.2(1)
Ga(3)–O(2)	1.937(3)	F(2)–Ga(3)–O(1)	88.7(1)
Ga(3)–F(2)	1.985(3)	O(9)–Ga(3)–O(7)	113.6(1)
		O(2)–Ga(3)–O(7)	87.0(1)
		F(2)–Ga(3)–O(7)	86.4(1)
		O(2)–Ga(3)–O(9)	90.1(1)
		F(2)–Ga(3)–O(9)	93.3(1)
		F(2)–Ga(3)–O(2)	173.4(1)

1,3-Diaminopropane

N(1)–C(1)	1.486(5)	N(1)–C(1)–C(3)	111.9(4)
N(2)–C(2)	1.484(5)	N(2)–C(2)–C(3)	111.6(4)
C(1)–C(3)	1.507(7)	N–H	0.95(4)
C(2)–C(3)	1.516(7)	C–H	0.97(4)

Distances between hydrogens and the anions (the shortest are in bold)

H(1)–O(12):	2.71(5)	H(2)–O(9):	2.76(5)	H(3)–O(7):	2.90(5)
H(4)–O(1):	2.61(4)	*H(5)–O(w)*[a]:	2.87(4)[a]	H(6)–O(8):	2.90(5)
H(7)–O(7):	**1.95**(3)	H(8)–F(1):	**2.08**(5)	H(9)–O(8):	**1.97**(4)
H(10)–O(9):	**2.40**(4)	H(11)–O(4):	**2.20**(3)	*H(12)–O(w)*[a]:	**1.86**(4)

Distance between the water molecule and the skeleton

O(w)–O(4):	2.958(4)	O(w)–O(8):	3.086(4)
O(w)–O(10):	3.037(4)	O(w)–F(2):	3.063(4)

---

[a] Corresponds to hydrogen bonds within the channel between the water and DAP molecules.

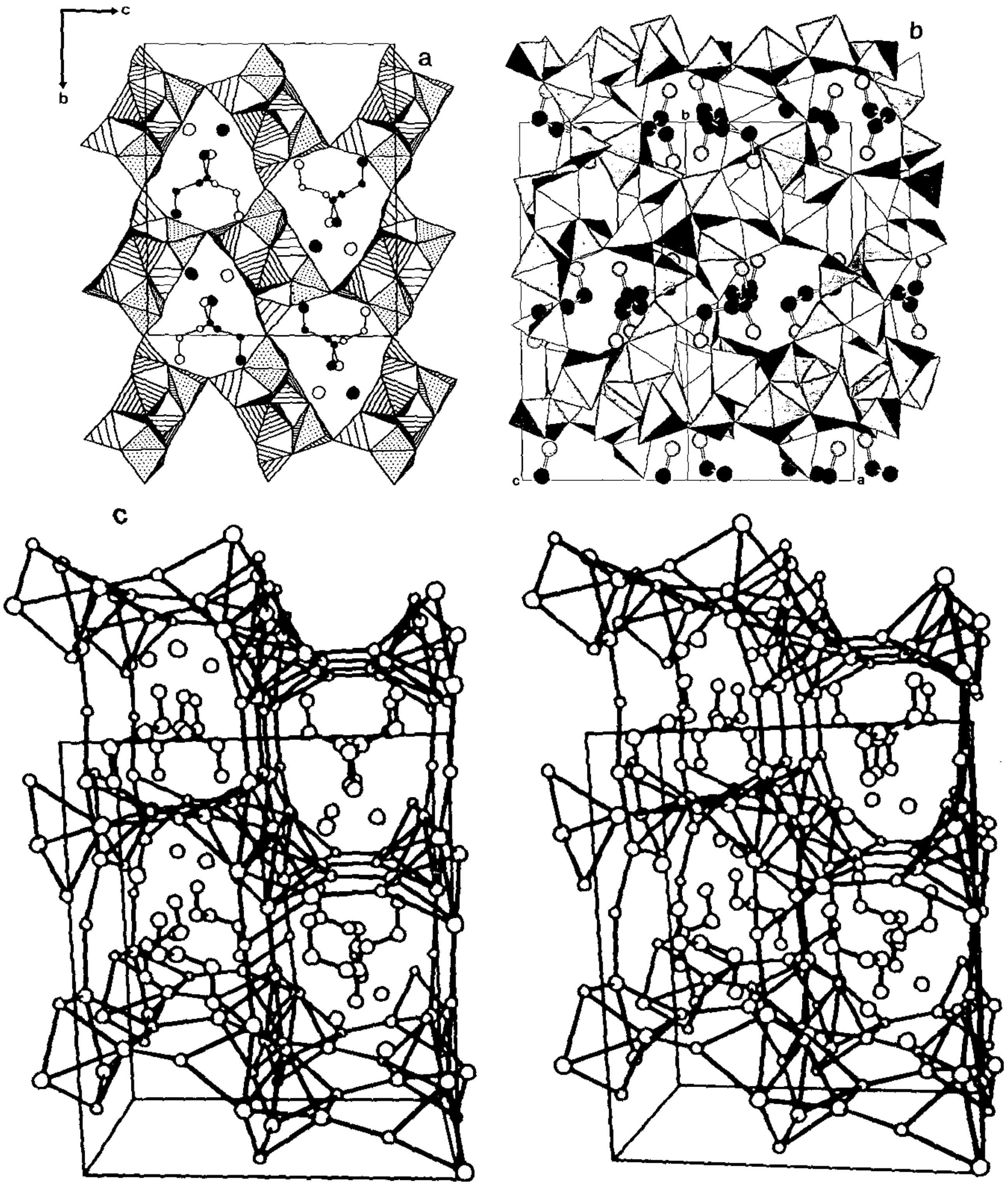

FIG. 2. (a) (100) projection of the structure of $Ga_3P_3O_{12}F_2$, $H_3N(CH_2)_3NH_3$, H_2O. The water molecule corresponds to the isolated circles. For the amine, hydrogen atoms have been omitted for sake of clarity. Small and medium circles refer to C and N atoms, respectively (white and black circles correspond to $x = 0$ and $\frac{1}{2}$, respectively). (b) View along [101], showing the eight-membered channels. (c) Stereoscopic view of the structure.

TABLE 5
Valence Bond Analysis of $Ga_3P_3O_{12}F_2$, $H_3N(CH_2)_3NH_3$, H_2O

	P(1)	P(2)	P(3)	Ga(1)	Ga(2)	Ga(3)	Σ
O(1)	1.18	—	—	—	—	0.70	1.88
O(2)	1.28	—	—	—	—	0.57	1.85
O(3)	1.22	—	—	—	0.74	—	1.96
O(4)	1.23	—	—	0.56	—	—	1.79
O(5)	—	1.26	—	—	0.75	—	2.01
O(6)	—	1.26	—	0.54	—	—	1.80
O(7)	—	1.22	—	—	—	0.69	1.91
O(8)	—	1.23	—	—	0.50	—	1.73
O(9)	—	—	1.20	—	—	0.67	1.87
O(10)	—	—	1.21	—	0.71	—	1.92
O(11)	—	—	1.27	0.54	—	—	1.81
O(12)	—	—	1.26	0.54	—	—	1.80
O(w)	—	—	—	—	—	—	—
F(1)	—	—	—	0.39	0.37	—	0.76
F(2)	—	—	—	0.41	—	0.37	0.78
Σ	4.91	4.97	4.94	2.98	3.07	3.00	

Note. The results refer to the equation $s = \exp[(R_0 - d)/0.37]$ (19) with $R_0 = 1.730$, 1.620, and 1.617 for Ga(O), Ga(F), and P, respectively.

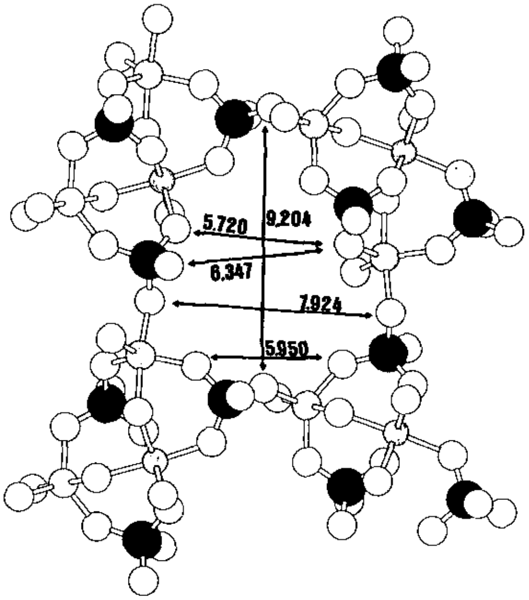

FIG. 3. Dimensions of the free aperture of the channel along [100].

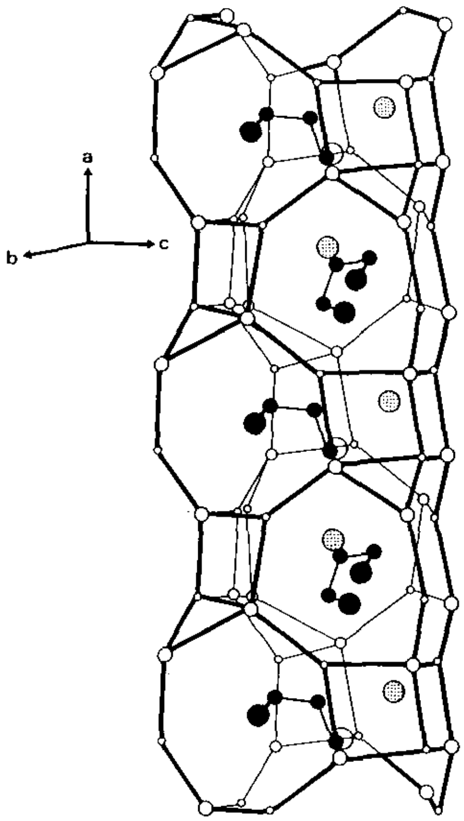

FIG. 4. Perspective view of the location of DAP and water (dipped circles) within the [100] channels. Only the Ga–P skeleton was represented (Ga, large circles; P, small circles). In the cage, the large empty circles correspond to one of the nitrogen atoms of the amine.

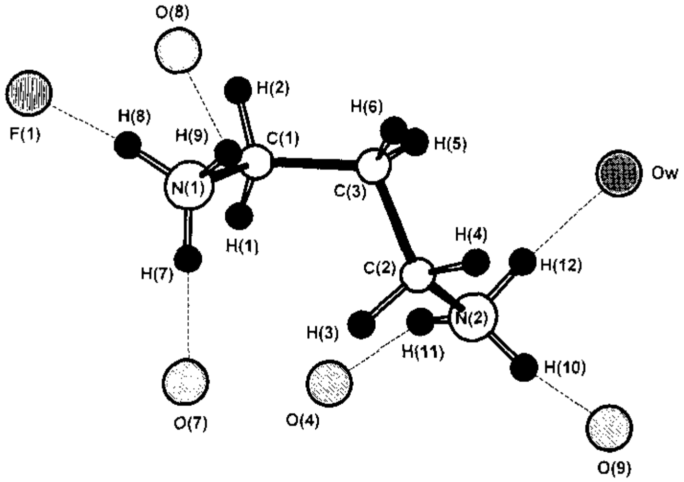

FIG. 5. Conformation of 1,3-diaminopropane in the structure. The strong hydrogen bonds are represented by dotted lines.

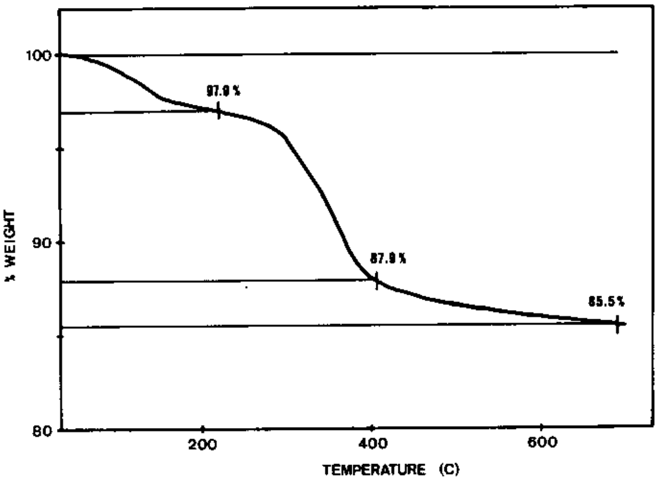

FIG. 6. TGA curve of $Ga_3P_3O_{12}F_2$, $H_3N(CH_2)_3NH_3$, H_2O.

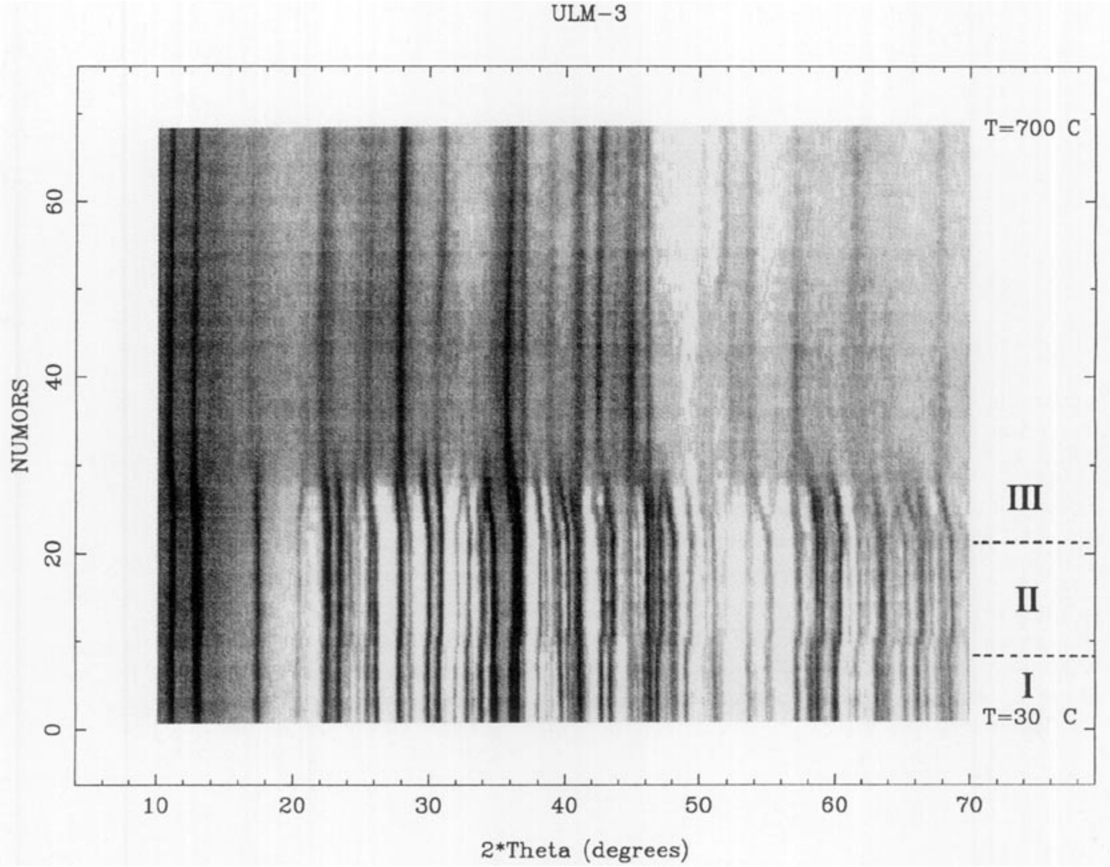

FIG. 7. Evolution of the X-ray powder pattern of $Ga_3P_3O_{12}F_2$, $H_3N(CH_2)_3NH_3$, H_2). The three domains described in the text are denoted I, II and III in the drawing.

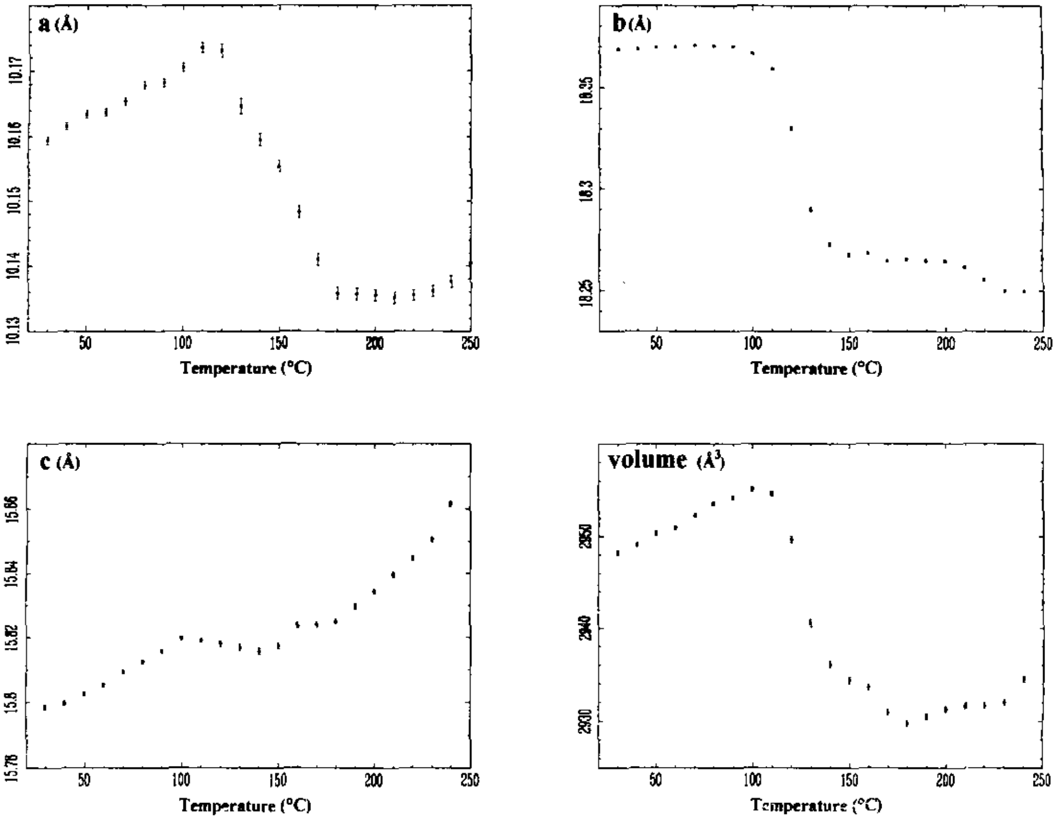

FIG. 8. Evolution of the cell parameters and volume with temperature.

REFERENCES

1. S. T. Wilson, B. M. Lok, C. A. Messina, T. R. Cannan, and E. M. Flanigen, *J. Am. Chem. Soc.* **104,** 1146 (1982).
2. E. M. Flanigen, R. L. Patton, and S. T. Wilson, *Stud. Surf. Sci. Catal.* **37,** 13 (1988).
3. T. E. Gier and G. D. Stuckey, *Nature* **349,** 508 (1991).
4. R. Xu, J. Chen, and C. Feng, *Stud. Surf. Sci. Catal.* **60,** 63 (1991).
5. J. L. Guth, H. Kessler, and R. Wey, *Stud. Surf. Sci. Catal.* **28,** 121 (1986).
6. J. L. Guth, H. Kessler, J. M. Higel, J. M. Lamblin, J. Patarin, A. Seive, J. M. Chezeau, and R. Wey, *ACS Symp. Ser.* **398,** 176 (1989).
7. H. Kessler, *MRS Symp. Ser.* **233,** 47 (1991).
8. M. Estermann, L. B. McCusker, C. Baerlocher, A. Merrouche, and H. Kessler, *Nature* **352,** 320 (1991).
9. P. Caullet, J. L. Guth, J. Hazm, J. M. Lamblin, and H. Gies, *Eur. J. Solid State Inorg. Chem.* **28,** 345 (1991).
10. D. Riou, T. Loiseau, and G. Férey, *J. Solid State Chem.* **102,** 4 (1992).
11. G. Férey, T. Loiseau, P. Lacorre, and F. Taulelle, *J. Solid State Chem.* **105,** 179 (1993).
12. T. Loiseau and G. Férey, *J. Chem. Soc. Chem. Comm.* 1197 (1992).
13. T. Loiseau and G. Férey, *Eur. J. Solid State Inorg. Chem.* **30,** 369 (1993).
14. J. Chen, L. Li, G. Yang, and R. Xu, *J. Chem. Soc. Chem. Comm.* 1217 (1989).
15. Th. Hahn (Ed.), "International Tables for X-Ray Crystallography," Kynoch Press, Birmingham, 1974. [Present Distributor: Kluwer Academic, Dortrecht, The Netherlands]
16. G. M. Sheldrick, *in* "Crystallographic Computing, 3" (G. M. Sheldrick, C. Krüger, and R. Goddard, Eds.), p. 175. Oxford Univ. Press, London, 1985.
17. G. M. Sheldrick, "SHELX-76, a Program for Crystal Structure Determination." University of Cambridge, 1976.
18. F. Taulelle, T. Loiseau, and G. Férey, unpublished results.
19. N. Brese and M. O'Keeffe, *Acta Crystallogr. Sect. B* **47,** 192 (1991).